Counting BPS states with scattering diagrams

Boris Pioline

LABORATOIRE DE PHYSIQUE THEORIQUE ET HAUTES ENERGIES

"Geometry meets physics - CY4 and beyond"

Woudschoten, Netherlands, 29/1/2025

BPS *dendroscopy* on local toric CY3

Boris Pioline

LPTHE
LABORATOIRE DE PHYSIQUE THEORIQUE ET HAUTES ENERGIES

cnrs

SORBONNE UNIVERSITÉ

"Geometry meets physics - CY4 and below"

Woudschoten, Netherlands, 29/1/2025

Based on 'BPS Dendroscopy on Local $\mathbb{P}^2$' [2210.10712]
and 'BPS Dendroscopy on Local $\mathbb{F}_0$' [2412.07680]

with Pierrick Bousseau, Pierre Descombes, Bruno Le Floch and Rishi Raj

Thanks to my wonderful co-authors



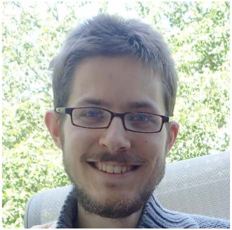


'BPS Dendroscopy on Local $\mathbb{P}^2$' [2210.10712]
'BPS Dendroscopy on Local $\mathbb{F}_0$' [2412.07680]

Pierrick Bousseau, Pierre Descombes, Bruno Le Floch and Rishi Raj

Introduction

- BPS states form a rich and tractable sector in string vacua with $\mathcal{N}=2$ supersymmetry. They saturate the BPS bound $M(\gamma) \geq |Z_z(\gamma)|$, where the central charge $Z_z \in \mathrm{Hom}(\Gamma, \mathbb{C})$ is linear in the electromagnetic charge, depending on the moduli z.
- As a result, BPS states preserve $\mathcal{N}=1$ supersymmetry, and are robust under variations of z. The BPS index $\Omega_z(\gamma)$ provides a microscopic underpinning of the entropy of BPS black holes.
- In type IIA string theory compactified on a CY3-fold X, BPS states are described by stable objects in the derived category of coherent sheaves $\mathcal{C} = D^b\mathrm{Coh}(X)$, with charge $\gamma = \mathrm{ch}\, E \in H_{\mathrm{even}}(X, \mathbb{Q})$.
- The BPS index coincides with the Donaldson-Thomas invariant $\Omega_\sigma(\gamma)$ with respect to a stability condition $\sigma \in \mathrm{Stab}\,\mathcal{C}$, restricted to the 'physical' slice $\sigma(z) \in \Pi \subset \mathrm{Stab}\,\mathcal{C}$, with $\Pi \sim \widetilde{\mathcal{M}_K}$.

Introduction

- $\Omega_\sigma(\gamma)$ is locally constant on $\mathrm{Stab}\,\mathcal{C}$, but can jump across real codimension one walls of marginal stability $\mathcal{W}(\gamma,\gamma')$, where the phases of the central charges $Z_\sigma(\gamma)$ and $Z_\sigma(\gamma')$ become aligned, making the decay $\gamma \to (\gamma') + (\gamma - \gamma')$ energetically possible.
- The jump of $\Omega_z(\gamma)$ across the wall is given by a universal wall-crossing formula *[Kontsevich Soibelman'08, Joyce Song'08]*. In the simplest 'primitive' case, with $\gamma'' := \gamma - \gamma'$,

$$\Omega_+(\gamma) - \Omega_-(\gamma) = \langle \gamma', \gamma'' \rangle \, \Omega(\gamma') \, \Omega(\gamma'')$$

  where $\langle -, - \rangle$ is the antisymmetrized Euler form, or Dirac pairing.
- When X admits a $\mathbb{C}^x$ action, one can define refined DT invariants $\Omega_\sigma(\gamma, y)$, reducing to usual DT as $y \to 1$. A similar WCF holds,

$$\Omega_+(\gamma, y) - \Omega_-(\gamma, y) = \frac{y^{\langle \gamma', \gamma'' \rangle} - y^{-\langle \gamma', \gamma'' \rangle}}{y - 1/y} \Omega(\gamma', y) \, \Omega(\gamma'', y)$$

Scattering diagrams

- Since BPS indices can only jump when the phases of the central charges of the constituents are aligned, it is convenient to analyze the BPS spectrum for fixed phase $\arg Z_\sigma(\gamma)$.
- For this purpose, define the scattering diagram $\mathcal{D}_\psi = \cup_\gamma \mathcal{R}_\psi(\gamma)$ as the union of the codimension 1 loci (or rays) in $\mathrm{Stab}\,\mathcal{C}$

$$\mathcal{R}_\psi(\gamma) = \{\sigma \in \mathrm{Stab}\,\mathcal{C}, \quad \Omega_\sigma(\gamma) \neq 0, \quad \arg Z_\sigma(\gamma) = \psi + \tfrac{\pi}{2}\}$$

and equip every point $z \in \mathcal{R}_\psi(\gamma)$ with an automorphism of the quantum torus algebra (or a suitable completion thereof),

$$\mathcal{U}_\sigma(\gamma) = \mathrm{Exp}\left(\frac{\Omega_\sigma(\gamma,y)}{y^{-1}-y}\mathcal{X}_\gamma\right) \ , \quad \mathcal{X}_\gamma \mathcal{X}_{\gamma'} = (-y)^{\langle\gamma,\gamma'\rangle}\mathcal{X}_{\gamma+\gamma'}$$

- Equivalently, take $\overline{\mathcal{U}}_\sigma(\gamma) = \exp\left(\frac{\bar\Omega_\sigma(\gamma,y)}{y^{-1}-y}\mathcal{X}_\gamma\right)$ where $\bar\Omega_\sigma(\gamma) := \sum_{k|\gamma} \frac{y-1/y}{k(y^k-y^{-k})}\Omega_\sigma(\frac{\gamma}{k}, y^k)$ are the 'rational' DT invariants.

Consistent scattering diagrams

- The WCF ensures that for any closed path $\sigma(t) : [0,1] \to \mathrm{Stab}\,\mathcal{C}$ intersecting the rays $\mathcal{R}_\psi(\gamma_i)$ at t_i, the ordered product is trivial:

$$\prod_i \mathcal{U}_{\sigma(t_i)}(\gamma_i)]^{\epsilon_i} = 1 \ , \quad \epsilon_i = \mathrm{sgn}\,\mathrm{Re}\left[e^{-\mathrm{i}\psi}\frac{\mathrm{d}}{\mathrm{d}t} Z_{\sigma(t_i)}\right]$$

- The WCF formula determines the BPS indices on outgoing rays ($\epsilon_i = 1$) in terms of BPS indices on incoming rays ($\epsilon_i = -1$). Locally, incoming rays 'scatter' to produce outgoing rays:

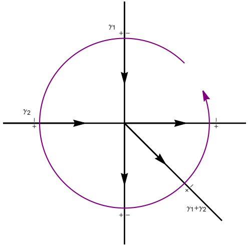

$$\begin{aligned} \mathcal{U}(\gamma_1)\mathcal{U}(\gamma_2) &= \mathcal{U}(\gamma_2)\mathcal{U}(\gamma_1+\gamma_2)\mathcal{U}(\gamma_1) \\ &\Downarrow \\ \Omega(\gamma_1+\gamma_2) &= \langle\gamma_1,\gamma_2\rangle\,\Omega(\gamma_1)\Omega(\gamma_2) \end{aligned}$$

Physics of scattering diagrams

- The rays $\mathcal{R}_\psi(\gamma_i)$ can be understood as walls of marginal stability for framed BPS states attached to an external probe with $Z(\gamma_\infty) = \mathrm{i}\rho e^{\mathrm{i}\psi}$, $\rho \to \infty$. The $\mathcal{U}(\gamma)$'s control jumps of framed DT invariants jumps, but conveniently encode unframed DT invariants.
- Along any two-dimensional slice, rays can be identified with gradient flow lines of $|Z_z(\gamma)| = \mathrm{Im}(e^{-\mathrm{i}\psi} Z_z(\gamma))$, oriented in the direction where $|Z(\gamma)|$ increases (opposite to attractor flow).
- Any ray $\mathcal{R}_\psi(\gamma)$ at any point z can be obtained (in multiple ways) by iterated scattering from a set of initial rays $\mathcal{R}(\gamma_i)$, as predicted by the Attractor Flow Tree Conjecture *[Denef Green Raugas'01, Denef Moore'07, Alexandrov BP'18, Argüz Bousseau '20, Mozgovoy'20]*

$$\bar{\Omega}_z(\gamma) = \sum_{\gamma=\sum \gamma_i} \frac{g_z(\{\gamma_i\}, y)}{\mathrm{Aut}(\{\gamma_i\})} \prod_i \bar{\Omega}_\star(\gamma_i, y)$$

where $g_z(\{\gamma_i\}, y)$ is a sum over attractor flow trees, and $\bar{\Omega}_\star(\gamma_i, y)$ are the (rational, refined) attractor invariants.

Outline

- In this talk, I will construct (part of) the scattering diagram for the simplest (yet non-trivial) examples of toric CY3-folds, namely $X = K_S$ for $S = \mathbb{P}^2$ and $S = \mathbb{F}_0 = \mathbb{P}^1 \times \mathbb{P}^1$.
- For such toric threefolds, $\mathcal{C} = D^b \operatorname{Coh} X$ is isomorphic to the derived category $D \operatorname{Rep}(Q, W)$ of representations for a certain quiver with potential. I shall first construct the scattering diagram $\mathcal{D}^Q$ in the 'quiver' region in $\operatorname{Stab} \mathcal{C}$, by identifying the set of initial rays / attractor invariants.
- Next I will discuss the large volume slice, where the central charge is given by the classical expression $Z_z(\gamma) = -\int_S e^{-zH} \operatorname{ch}(E)$.
- Finally, I will include corrections from worldsheet instantons and discuss the scattering diagram on the physical slice Π, interpolating between the quiver and LV scattering diagrams.

Scattering diagram for quivers

- Let (Q, W) a quiver with potential, $\gamma = (N_1, \dots, N_K) \in \mathbb{N}^{Q_0}$ a dimension vector and $\theta = (\theta_1, \dots, \theta_K) \in \mathbb{R}^{Q_0}$ a stability parameter (à la *[King'93]*) such that $(\theta, \gamma) := \sum N_i \theta_i = 0$.
- This data defines a supersymmetric quantum mechanics with 4 supercharges, gauge group $G = \prod_i U(N_i)$, superpotential W, FI parameters θ_i. SUSY ground states are harmonic forms on

$$\mathcal{M}_\theta(\gamma) = \{ \sum_{a:i\to j} |\Phi_a|^2 - \sum_{a:j\to i} |\Phi_a|^2 = \theta_i, \quad \partial_{\Phi_a} W = 0\}/G$$

- Mathematically, $\mathcal{M}_\theta(\gamma)$ is the moduli space of θ-semi-stable representations of (Q, W) (i.e. $(\theta, \gamma') \leq (\theta, \gamma)$ for any subrep) and the refined BPS index $\Omega_\theta(\gamma, y)$ is (roughly) its Poincaré polynomial.
- $\Omega_\theta(\gamma, y)$ may jump on real codimension 1 walls when the inequality is saturated (and on complex codimension 1 loci when W is varied, but we shall keep W fixed) .

Scattering diagram for quivers

- The BPS indices are conveniently encoded in the stability scattering diagram $\mathcal{D}(Q, W)$ *[Bridgeland'16]*, defined as the union of the real codimension-one rays $\{\mathcal{R}(\gamma), \gamma \in \mathbb{N}^{Q_0}\}$

$$\mathcal{R}(\gamma) = \{\theta \in \mathbb{R}^{Q_0} : (\theta, \gamma) = 0,\ \Omega_\theta(\gamma) \neq 0\}$$

- Each point along $\mathcal{R}(\gamma)$ is equipped with an automorphism of the quantum torus algebra,

$$\mathcal{U}_\theta(\gamma) = \mathrm{Exp}\left(\frac{\Omega_\theta(\gamma)}{y^{-1} - y} \mathcal{X}_\gamma\right) \ , \quad \mathcal{X}_\gamma \mathcal{X}_{\gamma'} = (-y)^{\langle \gamma, \gamma' \rangle} \mathcal{X}_{\gamma+\gamma'}$$

  where $\langle \gamma, \gamma' \rangle := \sum_{a: i \to j} (N_i N'_j - N_j N'_i)$.
- The WCF ensures that the diagram is consistent: for any generic closed path $\mathcal{P} : t \in [0, 1] \to \mathbb{R}^{Q_0}$, $\prod_i \mathcal{U}_{\theta(t_i)}(\gamma_i)^{\epsilon_i} = 1$

Attractor invariants for quivers

- Initial rays are defined as those containing the self-stability condition *[Manschot BP Sen'13; Bridgeland'16]*

$$(\theta_\star(\gamma), \gamma') = \langle \gamma', \gamma \rangle \quad \Leftrightarrow \quad \theta_i = - \sum_{a: i \to j} N_j$$

  Let $\Omega_\star(\gamma) := \Omega_{\theta_\star(\gamma)}(\gamma)$ be the attractor invariant. All other invariants are uniquely determined by consistency.

- Easy fact: For quivers without oriented loops, the only non-vanishing attractor invariants are supported on basis vectors associated to simple representations, $\Omega_\star(\gamma_i) = 1$. *[Bridgeland'16]*
- More generally, $\Omega_\star(\gamma) = 0$ unless the restriction Q' of Q to the support of γ is strongly connected (i.e. there is a path joining any pair of nodes in Q') *[Mozgovoy BP'20]*

Scattering diagram for Kronecker quiver

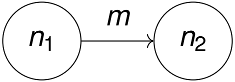

$$\theta_1 > 0, \theta_2 < 0 : \quad \dim \mathcal{M}_\theta(\gamma) = m n_1 n_2 - n_1^2 - n_2^2 + 1$$

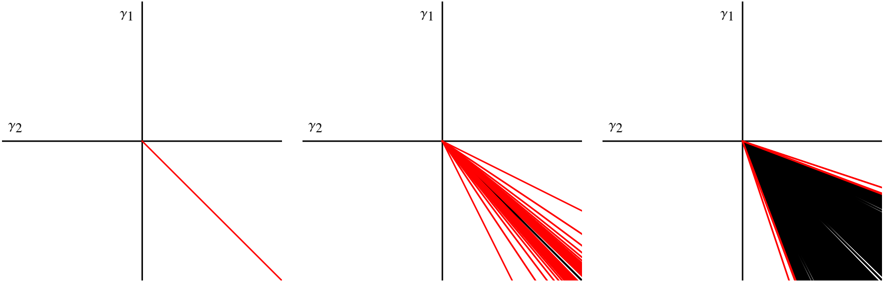

m=1 m=2 m=3

Quivers for local CY3

- Whenever a CY threefold X admits a (strong, full, cyclic) exceptional collection E, the category $D^b \operatorname{Coh} X$ is isomorphic to the category $D^b \operatorname{Rep}(Q, W)$ of representations of the quiver with potential associated to E. *[Bondal'90]*
- When X is toric, there is a simple prescription to obtain (Q, W) from brane tilings/periodic quivers. Eg. for $X = K_{\mathbb{P}^2}$,

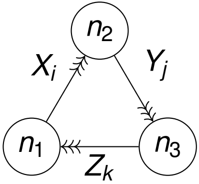

$$W = \sum \epsilon_{ijk} X_i Y_j Z_k$$

$$\begin{aligned} \gamma \quad &:= [r, c_1, \mathrm{ch}_2] \\ \gamma_1 \quad &= [-1, 0, 0] \\ \gamma_2 \quad &= [2, -1, -\tfrac{1}{2}] \\ \gamma_3 \quad &= [-1, 1, -\tfrac{1}{2}] \end{aligned}$$

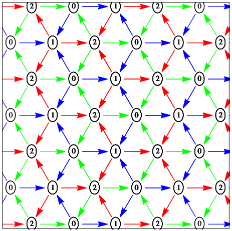

Attractor invariants for $K_{\mathbb{P}^2}$

- By studying expected dimension of the moduli space of semi-stable representations $\mathcal{M}_\theta(\gamma)$, *[Beaujard BP Manschot'20]* conjectured that for quivers associated to Ext-exceptional collections on local del Pezzo surfaces, the attractor index $\Omega_\star(\gamma)$ vanishes unless $\gamma = \gamma_i$ or γ lies in the kernel of the Dirac pairing, $\langle \gamma, - \rangle = 0$.
- This conjecture was tested and extended for general toric CY3 singularities in *[Mozgovoy BP '20, Descombes'21]*. It is now a theorem, at least for $X = K_{\mathbb{P}^2}$ and $K_{\mathbb{F}_0}$ *[Descombes]*.
- This allows to construct the quiver scattering diagram inductively, and to describe any BPS state in terms of attractor flow trees.

Quiver scattering diagram for $K_{\mathbb{P}^2}$

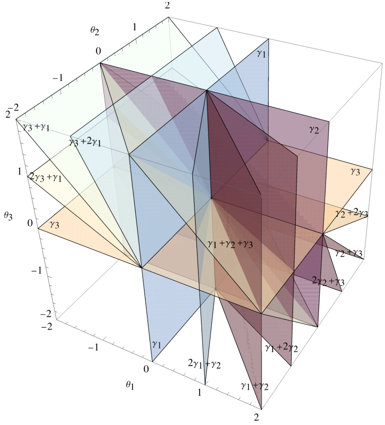

A 2D slice of the orbifold scattering diagram

Let $\mathcal{D}_o$ be the restriction of $\mathcal{D}(Q, W)$ to the hyperplane $\theta_1 + \theta_2 + \theta_3 = 1$:

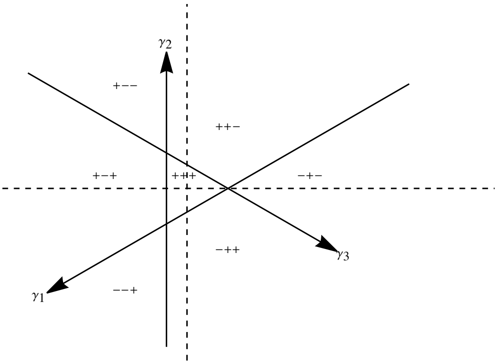

A 2D slice of the orbifold scattering diagram

Let $\mathcal{D}_o$ be the restriction of $\mathcal{D}(Q, W)$ to the hyperplane $\theta_1 + \theta_2 + \theta_3 = 1$:

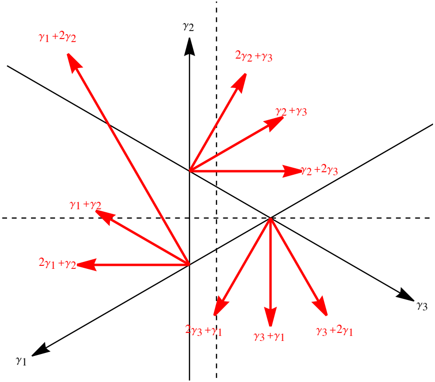

A 2D slice of the orbifold scattering diagram

The full scattering diagram $\mathcal{D}_o$ includes regions with dense set of rays:

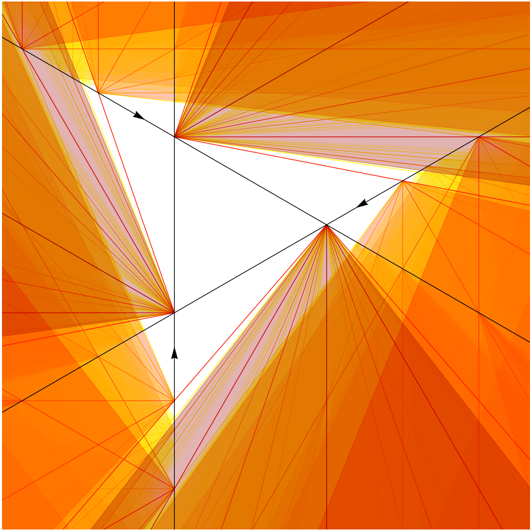

A 2D slice of the orbifold scattering diagram

The BPS index $\Omega_\theta(\gamma)$ for any γ can be obtained by listing scattering sequences, or attractor flow trees:

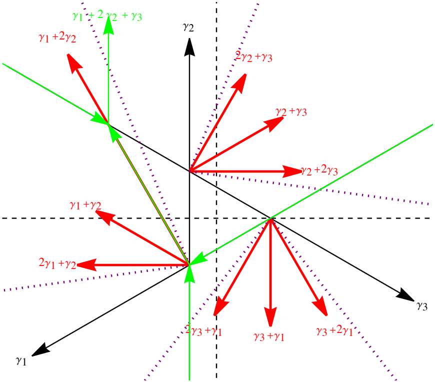

Bridgeland stability conditions

- More generally, Donaldson-Thomas invariants are defined in Bridgeland's framework of stability conditions on a triangulated CY3 category $\mathcal{C}$.
- A stability condition is a pair $\sigma = (Z, \mathcal{A})$ where $Z : \Gamma \to \mathbb{C}$ is a linear map and $\mathcal{A} \subset \mathcal{C}$ an Abelian subcategory (heart of t-structure) satisfying various axioms, e.g. $\mathrm{Im} Z(\gamma(E)) \geq 0 \; \forall E \in \mathcal{A}$.
- The space of stability conditions $\mathtt{Stab}\,\mathcal{C}$ is a complex manifold of dimension $\dim K(\mathcal{C}) = \dim H^{\mathrm{even}}_{cpt}(X)$. For $X = K_S$, $d = b_2(S) + 2$.
- $\mathtt{Stab}\,\mathcal{C}$ admits a (right) action by autoequivalences of $\mathcal{C}$, and a (left) action of $\widetilde{GL(2, \mathbb{R})}^+$ via orientation-preserving linear transf. of $(\mathrm{Re} Z, \mathrm{Im} Z)$, reducing the dimension to $b_2(S) = \dim \mathcal{M}_K$. The $\Omega_\sigma(\gamma)'s$ stay invariant, but the scattering diagram changes.

Scattering diagrams on triangulated categories

- As before, we define the scattering diagram $\mathcal{D}_\psi(\mathcal{C})$ as the union of codimension-one loci in $\mathrm{Stab}\,\mathcal{C}$,

$$\mathcal{R}_\psi(\gamma) = \{\arg Z_\sigma(\gamma) = \psi + \tfrac{\pi}{2}, \Omega_\sigma(\gamma) \neq 0\}\ , \quad \mathcal{U}_\sigma(\gamma) = \mathrm{Exp}\left(\frac{\Omega_\sigma(\gamma)}{y^{-1}-y}\mathcal{X}_\gamma\right)$$

  The WCF ensures that the diagram $\mathcal{D}_\psi(\mathcal{C})$ is locally consistent at each codimension-two intersection.

- In the 'quiver region' of $\mathrm{Stab}\,\mathcal{C}$ where the central charges $Z(E_i)$ of objects in an exceptional collection lie in a common half-plane, the heart σ coincides (up to tilt) with the Abelian category of quiver representations, and $\mathcal{D}_\psi(\mathcal{C})$ coincides with the quiver scattering diagram $\mathcal{D}(Q,W)$ upon setting $\theta_i = -\mathrm{Re}(e^{-\mathrm{i}\psi} Z(\gamma_i))$.
- For local CY3, this covers a finite region near the singular point, but not the large volume region.

Large volume scattering diagram for local $\mathbb{P}^2$

- Consider the large volume slice with central charge

$$Z^{\rm LV}_{(s,t)}(\gamma) = -\int_S e^{-(s+{\rm i}t)H}\,{\rm ch}\,E = -rT_D + dT - {\rm ch}_2$$

  with $T = s + {\rm i}t$, $T_D = \frac12 T^2$. Set $\psi = 0$ for simplicity.
- Since ${\rm Re}Z(\gamma) = \frac12 r(t^2 - s^2) + ds - {\rm ch}_2$, each ray $\mathcal{R}_0(\gamma)$ is contained in a branch of hyperbola asymptoting to $t = \pm(s - \frac{d}{r})$ for $r \neq 0$, or a vertical line $s = \frac{{\rm ch}_2}{d}$ when $r = 0$.
- Walls of marginal stability $\mathcal{W}(\gamma,\gamma')$ are nested half-circles centered on the real axis.

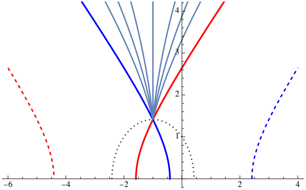

Large volume scattering diagram

- The objects $\mathcal{O}(m)$ and $\mathcal{O}(m)[1]$ for any $m \in \mathbb{Z}$ are known to be stable throughout the large volume slice *[Arcara Bertram'13]*. The corresponding rays are 45 degree lines ending at $s = m$.
- The region of validity of the orbifold exceptional collection (and its translates) covers the vicinity of the boundary at $t = 0$, hence those are the only initial rays. *[Bousseau'19]*.

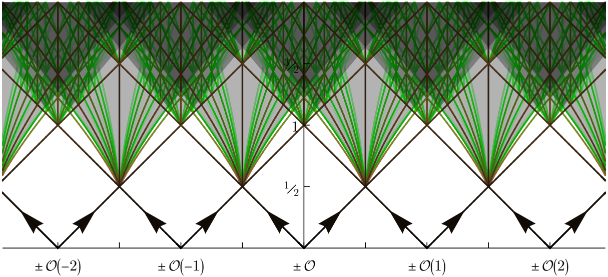

Scattering diagram in affine coordinates

Actually, Bousseau used different coordinates such that rays become line segments $rx + dy - \mathrm{ch}_2 = 0$. This works for any ψ:

$$x := \frac{\mathrm{Re}\left(e^{-\mathrm{i}\psi} T\right)}{\cos\psi}\,, \quad y := -\frac{\mathrm{Re}\left(e^{-\mathrm{i}\psi} T_D\right)}{\cos\psi} > -\frac{1}{2}x^2$$

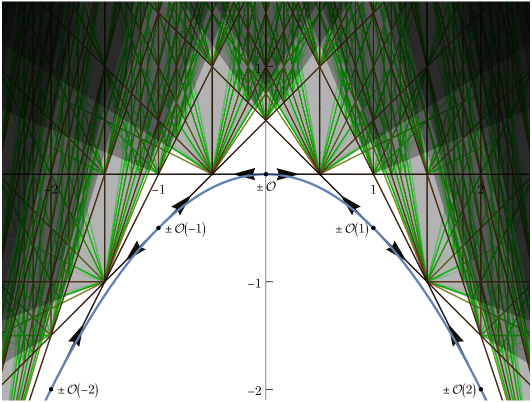

Flow tree formula at large radius

- This implies that all BPS states at large volume must arise as bound states of pure D4 and anti D4-branes. *How can one find the possible constituents for given γ and (s,t) ?*
- Think of $\mathcal{R}(\gamma)$ as the worldline of a fictitious particle of charge r, mass $M^2 = \frac{1}{2}d^2 - r\,\mathrm{ch}_2$ moving in a constant electric field. This makes it clear that constituents must lie in the past light cone.
- Moreover, the 'electric potential' $\varphi_s(\gamma) = d - sr = \mathrm{Im}Z(\gamma)/t$ increases along the flow. The first scatterings occur after each constituent $k_i\mathcal{O}(m_i)$ has moved by $|\Delta s| \geq \frac{1}{2}$, by which time $\varphi_s(\gamma_i) \geq |k_i|/2$.
- Since $\varphi_s(\gamma)$ is additive at each vertex, this gives a bound on the number and charges of constituents contributing to $\Omega_{(s,t)}(\gamma)$:

$$\sum_i k_i[1, m_i, \frac{1}{2}m_i^2] = \gamma\ , \quad s - t \leq m_i \leq s + t, \quad \sum_i |k_i| \leq 2\varphi_s(\gamma)$$

Flow trees for $\gamma = [1, 0, -3)$

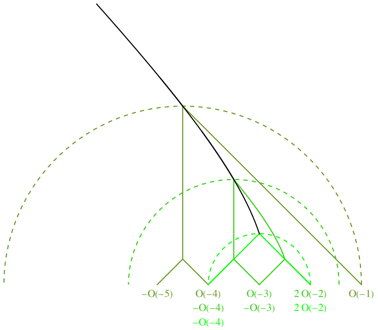

- $\{\{-\mathcal{O}(-5), \mathcal{O}(-4)\}, \mathcal{O}(-1)\}$
  $K_3(1,1)^2 \to 9$
- $\{\{-\mathcal{O}(-4), \mathcal{O}(-3)\}, \{-\mathcal{O}(-3), 2\mathcal{O}(-2)\}\}$
  $K_3(1,1)^2 K_3(1,2) \to 27$
- $\{-\mathcal{O}(-4), 2\mathcal{O}(-2)\}$
  $K_6(1,2) \to 15$

Total: $\Omega_\infty(\gamma) = 51 = \chi(\mathrm{Hilb}_4\mathbb{P}^2)$

Large volume scattering diagram for local $\mathbb{F}_0$

- For $S = \mathbb{P}^1 \times \mathbb{P}^1$, the space of stability conditions (modulo $GL(2,\mathbb{R})^+$) is parametrized by the Kähler moduli T_1, T_2. We focus on the canonical polarization where $\mathrm{Im}\, T_1 = \mathrm{Im}\, T_2$, and set $T_1 = T = s + \mathrm{i}t$, $T_2 = T + m$ with m real.
- The large volume slice is given by

$$Z^{\mathrm{LV}}_{x,t}(\gamma) = -rT(T+m) + d_1 T + d_2(T+m) - \mathrm{ch}_2$$

  The geometric rays are similar as for local $\mathbb{P}^2$, with $[r, d, \mathrm{ch}_2]$ replaced by $[2r, d_1 + d_2 - mr, \mathrm{ch}_2 - md_2]$. Set $\psi = 0$ for simplicity.
- The objects $\mathcal{O}(d_1, d_2)$, $\mathcal{O}(d_1, d_2)[1]$ are stable throughout the large volume slice *[Arcara Miles'14]*. The rays $\mathcal{R}_0(\mathcal{O}(d_1, d_2))$ start at $s = \min(d_1 - m, d_2)$ and bend to the left. Similarly, $\mathcal{R}_0(\mathcal{O}(d_1, d_2)[1])$ start at $s = \max(d_1 - m, d_2)$ and bend right.

- The category $D^b\,\mathrm{Coh}\,X$ is isomorphic to the derived category of representations for the quiver (Q, W) (or one of its mutations)

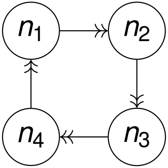

$$W = \sum_{\substack{(\alpha\beta)\in S_2\\(\gamma\delta)\in S_2}} \mathrm{sgn}(\alpha\beta)\,\mathrm{sgn}(\gamma\delta)\,\Phi_{12}^{\alpha}\,\Phi_{23}^{\gamma}\,\Phi_{34}^{\beta}\,\Phi_{41}^{\delta}$$

$$\begin{aligned}
\gamma &:= [r, d_1, d_2, \mathrm{ch}_2]\\
\gamma_1 &= [1, 0, 0, 0]\\
\gamma_2 &= [-1, 1, 0, 0]\\
\gamma_3 &= [-1, -1, 1, 1]\\
\gamma_4 &= [1, 0, -1, 0]
\end{aligned}$$

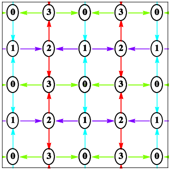

- The quiver (Q, W) is valid near the orbifold point Conifold$/\mathbb{Z}_2$.
- The validity of the mutated quiver (and its translates) near $t = 0$ ensure that the only initial rays in the large volume slice are $\mathcal{O}(d_1, d_2)$ and $\mathcal{O}(d_1, d_2)[1]$ *[Le Floch BP Raj'24]*

Initial rays for local $\mathbb{F}_0$ at large volume

In (x, t) coordinates, $\psi = 0$, $m = 1/2$:

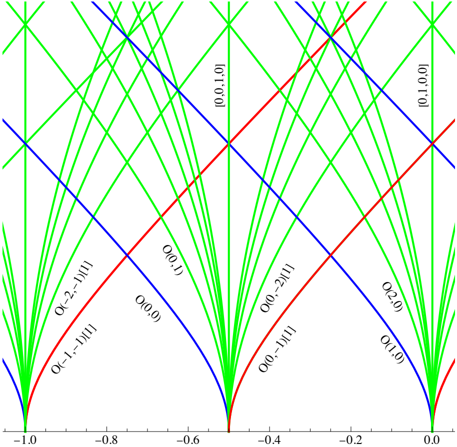

Initial rays for local $\mathbb{F}_0$ at large volume

In (x, y) coordinates, $\psi = 0$, $m = 1/2$:

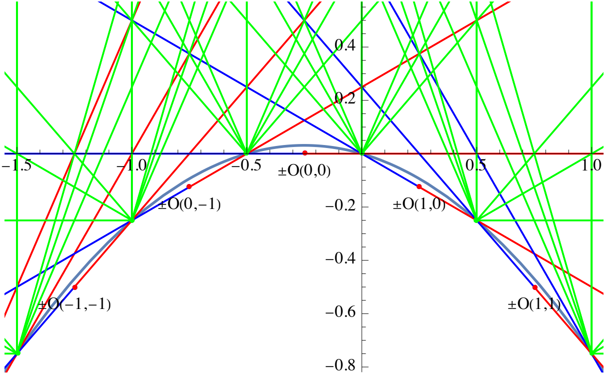

The infinite sets of rays originating from $s \in \mathbb{Z}$ and $s = \mathbb{Z} - m$ come from the scattering of two rays $\mathcal{R}(\gamma_1), \mathcal{R}(\gamma_2)$ with $\langle \gamma_1, \gamma_2 \rangle = 2$ below the parabola !

Kähler moduli space

- Mirror symmetry selects a particular Lagrangian subspace $\Pi \subset \mathrm{Stab}\,\mathcal{C}$ in the space of Bridgeland stability conditions.
- For local del Pezzo surfaces, the mirror CY3 is (a conic bundle over) a genus one curve Σ. The D2 and D4 central charges (T_i, T_D) are given by periods of a holomorphic differential with logarithmic singularities, and satisfy Picard-Fuchs equations.
- Rather than working with flat coordinates T_i, it is advantageous to use (τ, m_i) where τ parametrizes the Coulomb branch while m_i are gauge couplings/mass parameters in the 5D gauge theory.
- Near the large volume point, mirror symmetry ensures that $Z(\gamma) \sim -\int_S e^{-J}\,\mathrm{ch}(E)$, up to Todd-class and worldsheet instantons which may be absorbed by $\widetilde{GL(2,\mathbb{R})^+}$.

Modularity in Kähler moduli space

- In some cases, the monodromy group is a subgroup $\Gamma \subset SL(2,\mathbb{Z})$, and the universal cover of $\mathcal{M}_K = \mathbb{H}/\Gamma$ becomes the Poincaré half-plane $\mathbb{H}$. *[Closset Magureanu'21; Aspman Furrer Manschot'21]*
- This happens for $X = K_{\mathbb{P}^2}$, where $\Gamma = \Gamma_1(3)$, and for $X = K_{\mathbb{F}_0}$ at special points $m \in \mathbb{Z}$ where $\Gamma = \Gamma_0(8)$. For generic m, $\Gamma = \Gamma_1(4)$ with a square root branch cut.

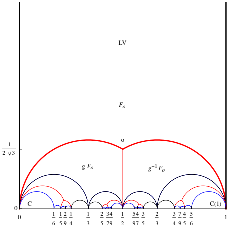

$K_{\mathbb{P}^2} : \Gamma_1(3)$

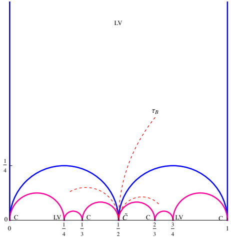

$K_{\mathbb{F}_0} : \Gamma_1(4)$

Central charge as Eichler integral

- $(\partial_\tau T, \partial_\tau T_D)$ are proportional to the periods $(1,\tau)$ of the mirror curve. Integrating along a path from reference point o to τ, one finds an Eichler integral representation

$$\boxed{\begin{pmatrix} T \\ T_D \end{pmatrix}(\tau) = \begin{pmatrix} T \\ T_d \end{pmatrix}(\tau_o) + \int_{\tau_o}^{\tau} \begin{pmatrix} 1 \\ u \end{pmatrix} C(u)\,\mathrm{d}u}$$

where $C(\tau)$ is a weight 3 modular form:

$$C_{\mathbb{P}^2} = \frac{\eta(\tau)^9}{\eta(3\tau)^3}, \quad C_{\mathbb{F}_0} = \frac{\eta(\tau)^4\eta(2\tau)^6}{\eta(4\tau)^4}\sqrt{\frac{J_4+8}{J_4+8\cos\pi m}}$$

Here $J_4(\tau) = 8 + \left(\frac{\eta(\tau)}{\eta(4\tau)}\right)^8$ is the Hauptmodul for $\Gamma_1(4)$. This provides an computationally efficient analytic continuation of Z_τ.

Π-scattering diagram for local $\mathbb{P}^2$

- The scattering diagram $\mathcal{D}^{\Pi}_{\psi}$ along the physical slice should interpolate between $\mathcal{D}^{\rm LV}_{\psi}$ around $\tau = i\infty$ and $\mathcal{D}_o$ around $\tau = \tau_o$, and be invariant under the action of $\Gamma_1(3)$.
- Under $\tau \mapsto \frac{\tau}{3n\tau+1}$ with $n \in \mathbb{Z}$, $\mathcal{O} \mapsto \mathcal{O}[n]$. Hence there is a doubly infinite family of initial rays emitted at $\tau = 0$, associated to $\mathcal{O}[n]$.

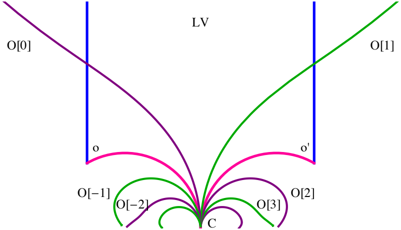

- Similarly, there must be an infinite family of initial rays coming from $\tau = \frac{p}{q}$ with $q \neq 0 \mod 3$, corresponding to $\Gamma_1(3)$-images of $\mathcal{O}$, where an object denoted by $\mathcal{O}_{p/q}$ becomes massless.

Π-scattering diagram for small ψ

- For $|\psi|$ small enough, the only rays which reach the large volume region are those associated to $\mathcal{O}(m)$ and $\mathcal{O}(m)[1]$. Thus, the scattering diagram $\mathcal{D}^{\Pi}_{\psi}$ is isomorphic to $\mathcal{D}^{\rm LV}_{\psi}$ inside $\mathcal{F}$ and its translates:

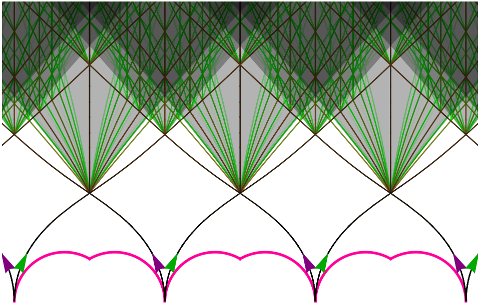

Scattering diagram in affine coordinates

- In affine coordinates $(x, y) = \left(\frac{\mathrm{Re}\left(e^{-\mathrm{i}\psi} T\right)}{\cos\psi}, -\frac{\mathrm{Re}\left(e^{-\mathrm{i}\psi} T_D\right)}{\cos\psi} \right)$, the initial rays $\mathcal{R}_\psi(\mathcal{O}(m))$ are still tangent to the parabola $y = -\frac{1}{2}x^2$ at $x = m$, but the origin of each ray is shifted to $x = m + \mathcal{V}\tan\psi$ where $\mathcal{V}$ is the quantum volume

$$\mathcal{V} = \mathrm{Im}\, T(0) = \frac{27}{4\pi^2} \mathrm{Im}\left[\mathrm{Li}_2(e^{2\pi\mathrm{i}/3})\right] \simeq 0.463$$

- The topology of $\mathcal{D}^{\Pi}_{\psi}$ jumps at a discrete set of rational values

$$\mathcal{V}\tan\psi \in \{\tfrac{F_{2k}+F_{2k+2}}{2F_{2k+1}}, k \geq 0\} = \{\tfrac{1}{2}, 1, \tfrac{11}{10}, \tfrac{29}{26}, \tfrac{19}{17}, \dots\}$$

and a dense set of values in $[\frac{\sqrt{5}}{2}, +\infty)$ where secondary rays pass through a conifold point.

Affine scattering diagram, $|\mathcal{V} \tan\psi| < 1/2$

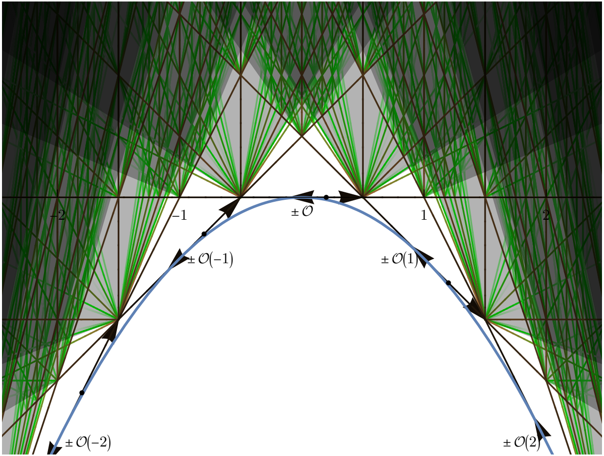

Π-scattering diagram, $\psi = 0$

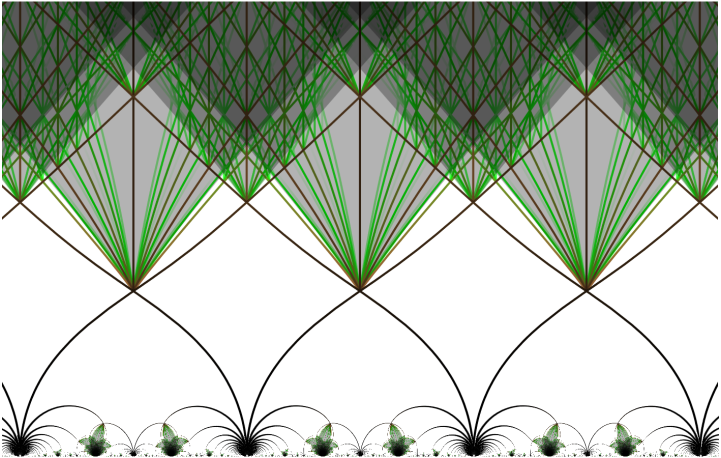

Π-scattering diagram, $\psi = 0.3$

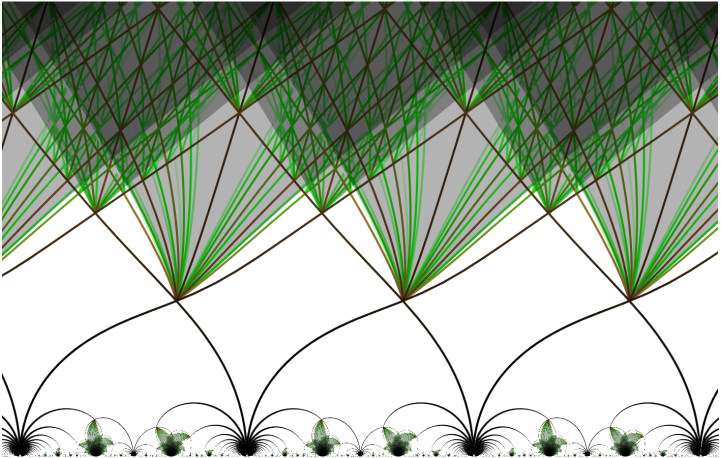

Π-scattering diagram, $\psi = 0.6$

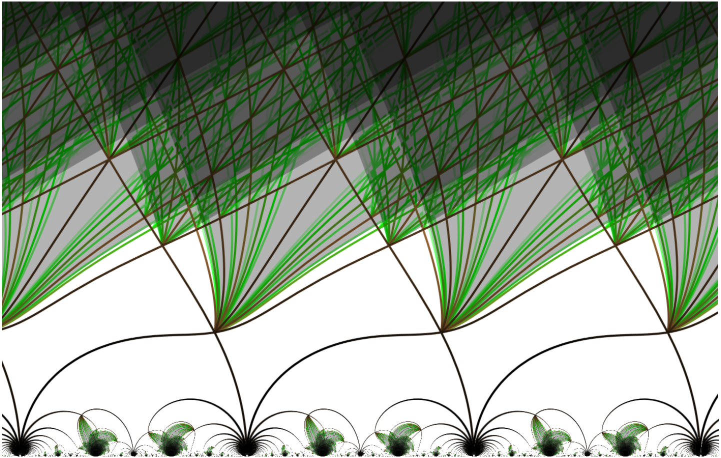

Π-scattering diagram, $\psi = 0.8$

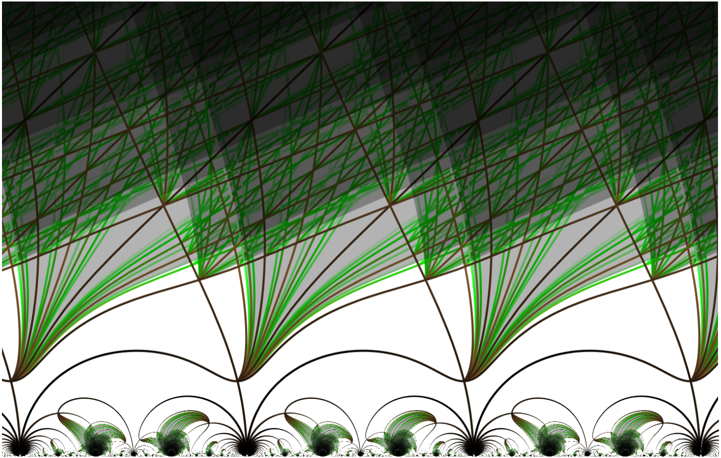

Π-scattering diagram, $\psi = 0.824$

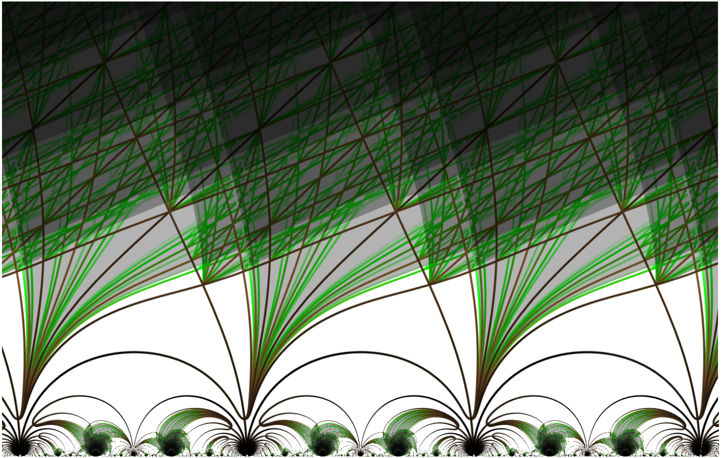

Π-scattering diagram, $\psi = 0.825$

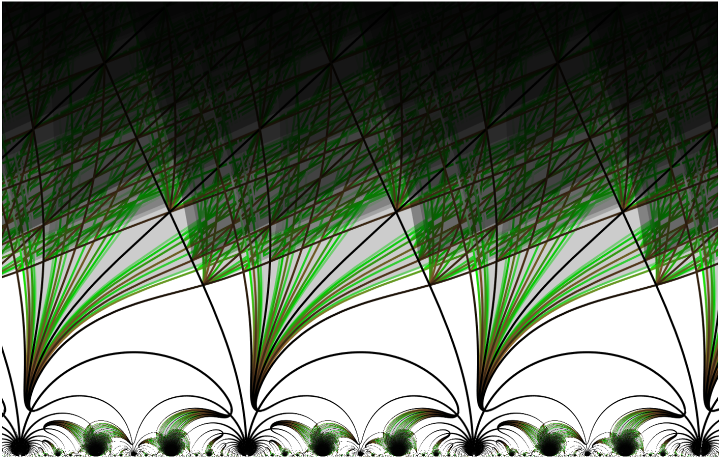

Π-scattering diagram, $\psi = 0.9$

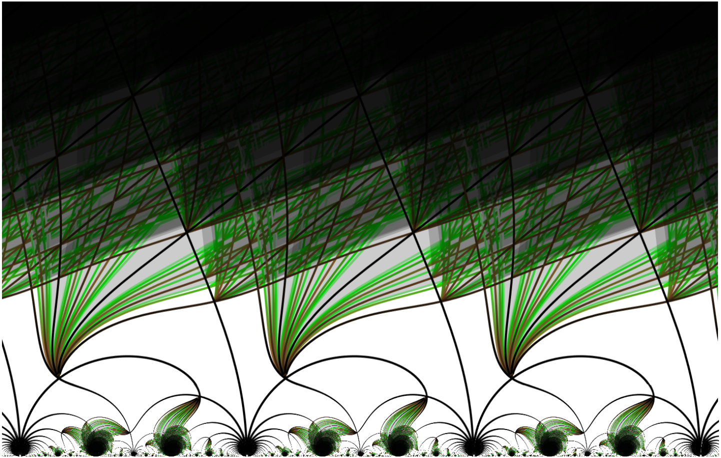

Π-scattering diagram, $\psi = 1$

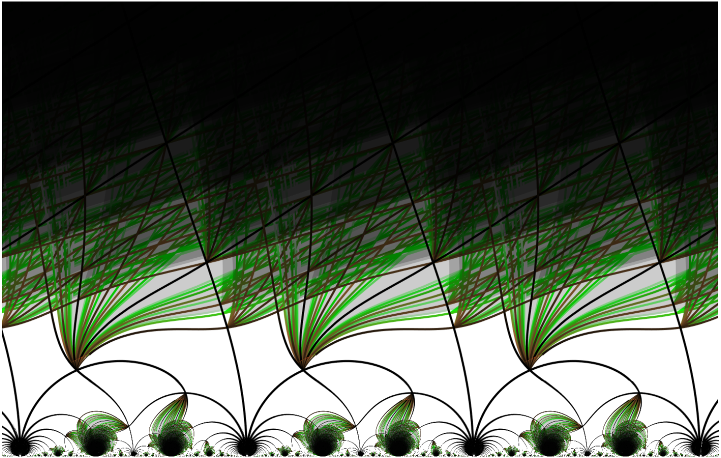

Π-scattering diagram, $\psi = 1.137$

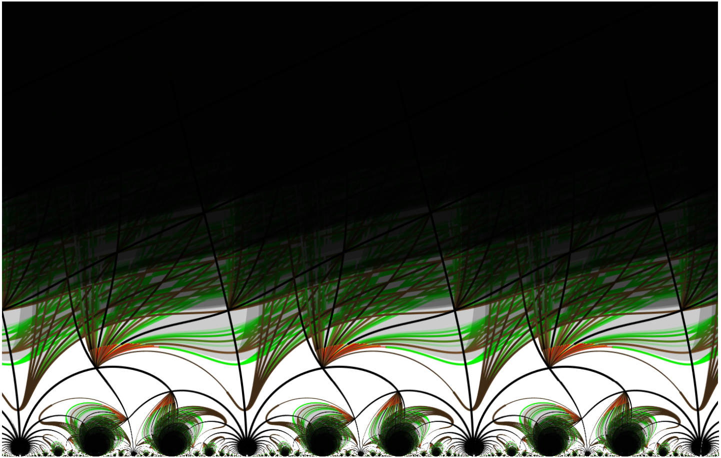

Π-scattering diagram, $\psi = 1.139$

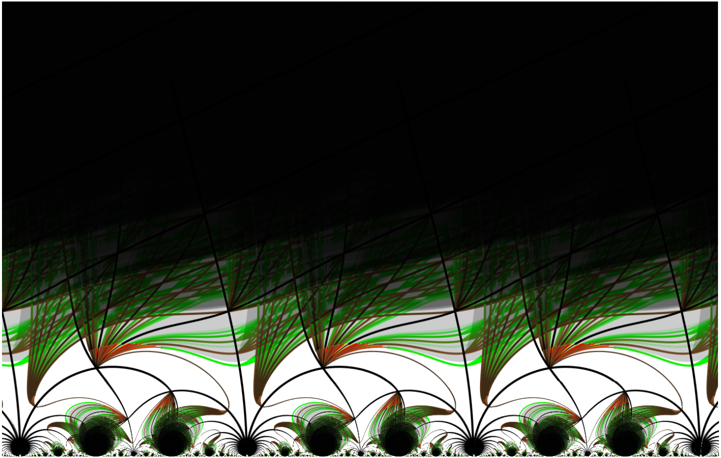

Π-scattering diagram, $\psi = \pi/2$

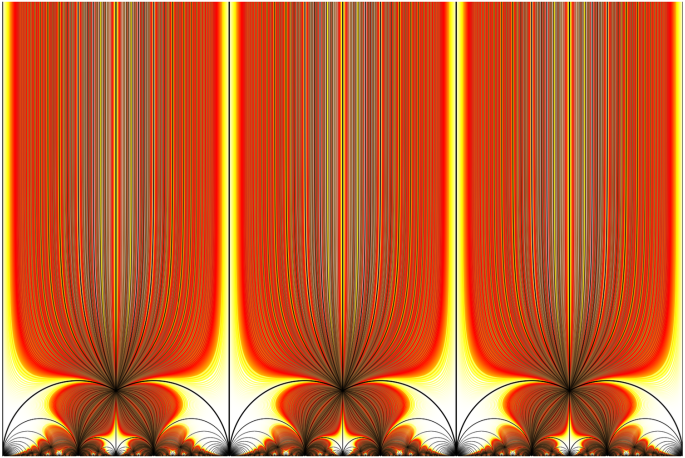

Π-scattering diagram for $\psi = \pm\frac{\pi}{2}$

- For $\psi = \pm\frac{\pi}{2}$, the geometric rays $\{\mathrm{Im} Z_\tau(\gamma) = 0\}$ coincide with lines of constant ratio $\frac{\mathrm{Im}\, T_D}{\mathrm{Im}\, T} = \frac{d}{r}$, independent of ch_2:

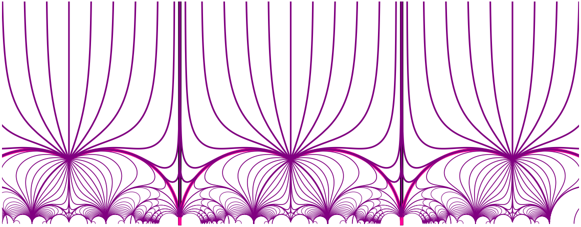

- Hence, there is no wall-crossing between τ_o and $\tau = \mathrm{i}\infty$ when $-1 \leq \frac{d}{r} \leq 0$, explaining why the Gieseker index $\Omega_\infty(\gamma)$ agrees with the quiver index $\Omega_c(\gamma)$ in the anti-attractor chamber.

Douglas Fiol Romelsberger'00, Beaujard BP Manschot'20

Π-scattering diagram for $K_{\mathbb{F}_0}$

- For local $\mathbb{F}_0$, the Π-scattering diagram is complicated by branch cuts and m-dependence. The quantum volume is now

$$T(0,m) = \mathrm{i}\mathcal{V}(m) = \frac{2}{\pi^2}\left(\mathrm{Li}_2(\mathrm{i}e^{\mathrm{i}\pi m/2}) - \mathrm{Li}_2(-\mathrm{i}e^{\mathrm{i}\pi m/2})\right)$$

- In (x,y) coordinates, the origin of the initial rays is shifted by $\Delta x = \tan\psi\,\mathrm{Re}\mathcal{V}(m) - \mathrm{Im}\mathcal{V}(m)$. For Δx small enough, the topology is the same as for the LV diagram: (here $m = 0.4, \psi = 0.4$)

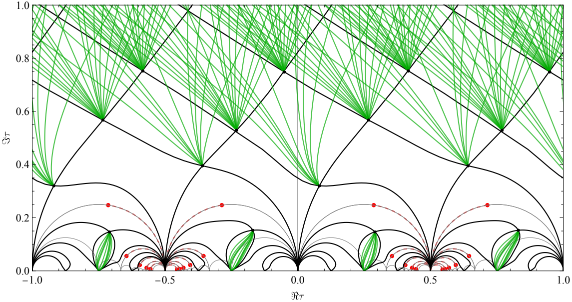

Large volume scattering diagram for $K_{\mathbb{F}_0}$

- As ψ increases, some of the initial rays curl back to $\Gamma_0(4)$ images of the LV point, while suitable homological shifts escape to infinity: (here $m = 0.4, \psi = 0.98$)

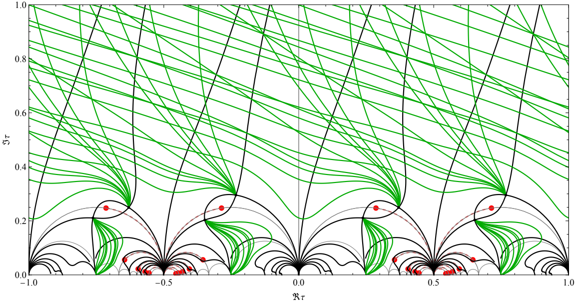

Large volume scattering diagram for $K_{\mathbb{F}_0}$

- The region around the branch point reproduces the quiver scattering diagram, after unfolding:

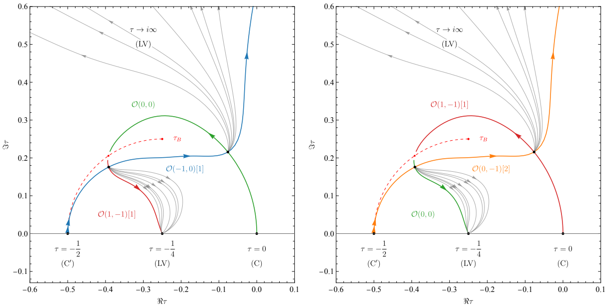

Conclusion - outlook

- Scattering diagrams provide an efficient way to organize the (unframed) BPS spectrum on local CY3 manifolds, and suggests a natural decomposition into elementary constituents. What does it mean mathematically?
- The framed BPS invariants are constant in the complement of the scattering diagram. It would be interesting to see how they interpolate between DT/PT invariants at large volume and plane partition counts near the orbifold point.
- One could try to use the same techniques for toric CY4 singularities, for example K_X where X is one of the 18 smooth toric Fano 3-folds, such as $\mathbb{P}^3, \mathbb{P}^2 \times \mathbb{P}^1, \mathbb{P}^1 \times \mathbb{P}^1 \times \mathbb{P}^1$...

Scattering diagrams for toric CY4 ?

- The dynamics of a D1-brane probing the CY4 singularity is described by a $(0,2)$ quiver gauge theory, with vector, chiral and Fermi multiplets and relations (Q, J, E) encoded in a 3D-periodic tiling, or brane brick *[Franco Ghim Lee Seong, Yokoyama'15,Franco Seong'22]*.
- These models presumably arise from strong full exceptional collections of line bundles on X constructed in *[Bernardi Tirabassi'10]*, or mutations thereof, corresponding to trialities in the (0,2) gauge theory *[Gadde Putrov Gukov'13]*.
- The Witten index of the quiver gauge theory is computable by localization, provided the superpotential is generic *[Hori Kim Yi'14]*. What is its precise interpretation in DT4 theory ?
- Presumably DT4-invariants can be encoded in a scattering diagram, with rays equipped with an automorphism of Joyce's vertex Lie algebra. Can one use this to say something about moduli spaces of Gieseker-stable sheaves on Fano threefolds ?

Thanks for your attention !